Tuning dynamic DNA- and peptide-driven self-assembly in DNA-peptide conjugates.

Emerald R. Taylor,[a] Akiko Sato,[a] Prashant G. Gudeangadi,[a] David M. Beal,[b] James A. Hopper,[a] Michael R. Reithofer*[c] and Christopher J. Serpell*[a]

[a] School of Physical Sciences, Ingram Building, University of Kent, Canterbury, Kent, CT2 7NH, UK
[b] School of Biosciences, Stacey Building, University of Kent, Canterbury, Kent, CT2 7NJ, UK
[c] Department of Inorganic Chemistry, University of Vienna, Währinger Straße. 42, 1090 Vienna, Austria

DNA-peptide conjugates offer an opportunity to marry the benefits of both biomolecules, such as the high level of control and programmability found with DNA and the chemical diversity and biological stability of peptides. These hybrid systems offer great potential in fields such as therapeutics, nanotechnology, and robotics to name a few. Using the first DNA-β-turn peptide conjugate, we present three studies designed to investigate the self-assembly of DNA-peptide conjugates over a period of 28 days. Time-course studies, such as these have not been previously conducted for DNA-peptide conjugates, although they are common in pure peptide assembly, for example in amyloid research. By using aging studies to assess the structures produced, we gain insights into the dynamic nature of these systems. The first study explores the influence varying amounts of DNA-peptide conjugates have on the self-assembly of our parent peptide. Study 2 explores how DNA and peptide can work together to change the structures observed during aging. Study 3 investigates the presence of orthogonality within our system by switching the DNA and peptide control on and off independently. These results show that two orthogonal self-assemblies can be combined and operated either independently or in tandem within a single macromolecule, with both spatial and temporal effects upon the resultant nanostructures.

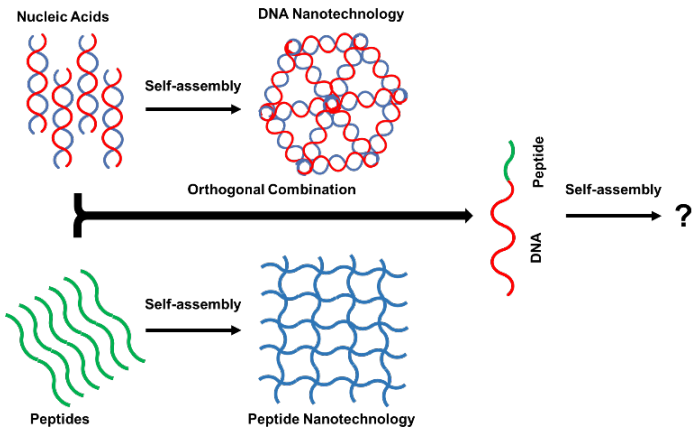

Introduction

Biomolecular chemistry opens up a wide array of applications in the marrying of biology and chemistry.[1] DNA and peptides in particular offer differing properties in their supramolecular chemistry. DNA has highly site-specific recognition driven through Watson-Crick base pairing and the formation of the double helix; this can be manipulated to achieve more complex structures, such as those explored in DNA nanotechnology.[2] Peptides, with a large library of amino acids have a high level of variation and self-assembly motifs, giving more diversity and fluidity of structure.[3–6] DNA-peptide conjugates therefore exploit the properties of each of their components, but also overcome their individual weaknesses. For example, peptides can benefit from the rigid self-assembly control that DNA provides, while DNA also benefits from the increased stability in biology and cell penetration which peptides provide.[1,7] This makes DNA-peptides ideal candidates for exploration into medicinal and therapeutic fields,[6,8,9] as well as nanoscale control and assembly.[5]

DNA-peptide conjugate systems have recently been rising in prominence. Buchberger et al. explored the nanoscale assembly of DNA origami blocks connected via coiled-coil peptides to yield controllable nanostructures. By varying the number of handles the team controlled assembly to yield, dimers, trimers and nanofibers.[1] Diphenylalanine nucleic acid conjugates have been shown to self-assembly nanoparticles.[10] The nanoscale control of these systems has been explored through external stimuli such as salt, pH, concentration and heat.[2,11,12] Self-assembly has been driven through the DNA or peptide components, or jointly.[13–15] In general, a hierarchical approach has been used in which pre-assembled DNA or peptide units which interlinked via peptide or DNA directed assembly, respectively.[7,16] The aging of self-assembled structures has not been explored in the DNA-peptide conjugate field. However, it is well established in amyloid peptide structural studies.[17] Studying the way that amyloid proteins and peptides self-assemble over time greatly increases the knowledge and insight which can be gained from these amyloid fibres.[18–20] These same insights can be beneficial to the study and understanding of DNA-peptide self-assembly, as well as allowing the exploration of the dynamic nature that could be present within these systems.[21–23]

We here report the first conjugates of DNA and β-turn-forming peptides, and show how their self-assembly in space and time is influenced by each of the components separately and together.

Results and Discussion

Our system is comprised of two complementary DNA sequences modified with a bifunctional crosslinker and attached by copper-free click reaction to the β-turn ultrashort peptide, N_3-ILVAGK-NH_2. ILVAGK is an ultrashort peptide with a hydrophobic block proceeded by increasingly hydrophilic residues.[24,25] This gives ILVAGK its amphiphilic character which promotes a progressive self-assembly from random coil to

α–coiled and finally β–turn confirmations. ILVAGK shows a greater range of structures when compared with other peptides.[26] This peptide is pH and salt sensitive and known to self-assemble to form hydrogel systems, with potential use in medicine.[27]

Complementary oligonucleotides **A**, and **A'** 15-mers with a poly-T 5-mer spacer, and a C-6 primary amine terminated modification, were purchased (ESI for Sequences). Several experiments were conducted to obtain a suitable linker for our DNA-peptide conjugates. Success was achieved with *N*-hydroxysuccinimide (NHS) ester-based maleimide and cyclooctyne linkages, and for this paper we focus on the cyclooctyne cross-linked DNA-peptide conjugates. Oligonucleotides (**A-NH_2** and **A'-NH_2**) were first modified with bicyclononyne (**BCN**) activated with NHS through carbamate-mediated amide coupling.[28] **BCN-NHS** a bifunctional linker, was dissolved in dimethylformamide (DMF) and added to oligonucleotides in phosphate buffer, before being heated to 37 °C for 2 hours. Crude BCN-oligonucleotides were purified by size exclusion chromatography before DNA–peptide conjugation. **A-BCN** and **A'-BCN** were conjugated to **N_3–ILVAGK–NH_2** (see ESI for preparation) through strain promoted alkyne-azide click reaction (SPAAC) (Fig.1).[29] Oligonucleotide–peptide conjugates were purified by anion exchange and size exclusion chromatography before a successful conjugation was confirmed by polyacrylamide gel electrophoresis (PAGE) and mass spectrometry. Masses were observed for DNA–peptide conjugates at 7150.61 $[M+H^+]^+$ and 7128.63 Da $[M+H^+]^+$ for **A-ILVAGK** and **A'–ILVAGK**, respectively. (See ESI Fig. S4 and 5).

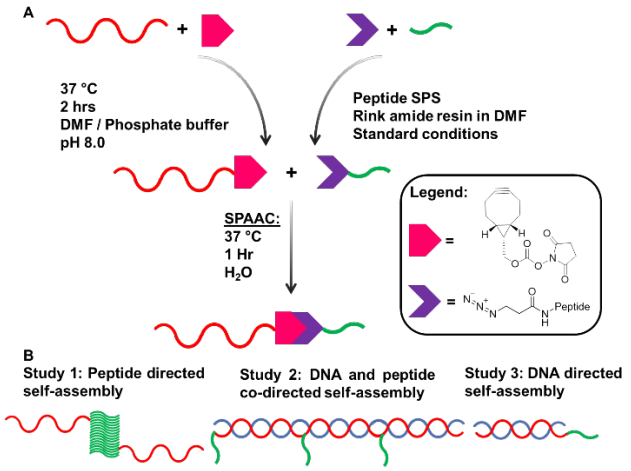

Figure 1. A: Schematic representation of synthesis pathway to achieve DNA–peptide conjugates by solution phase modification. B: Schematic representation of studies 1, 2 and 3.

Three studies were conducted to investigate how the self-assembly of this system changes when driven by peptide and/or DNA self-assembly, Study 1 explored the way in which DNA–peptide conjugates affected the self-assembly of the parent peptide, **ILVAGK**. DNA hybridisation was added as a second driving force in Study 2, modulating and linking prior substructures. Finally, Study 3 investigated whether the two self-assembling systems were orthogonal by switching each type of assembly on and off. The studies were monitored over a period of 28 days to observe the dynamic nature of this system and investigate the stability of the self-assemblies produced. To our knowledge this is the first study which investigates the self-assembly of DNA-peptide conjugates over an extended period. The ability of the DNA-peptide conjugate to self-assemble was analysed over time by atomic force microscopy (AFM), dynamic light scattering (DLS) and circular dichroism (CD). A variety of nanostructures were observed, which we have classified as the following morphologies; small and large flakes, fibre-like, fractal-like, dot-like and network-like (Fig. S1).[30]

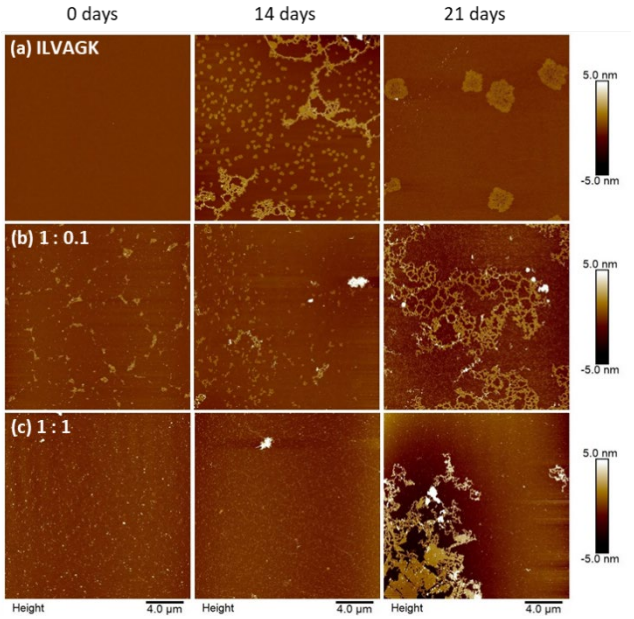

Figure 2. AFM images showing change in self-assembly of **ILVAGK** (a) **ILVAGK** doped with varying amounts of **A'-ILVAGK** DNA-peptide conjugate (1 : 0.1 (b) and 1 : 1 (c)), over 28 days of aging in TAMg buffer (see supplementary Fig. S9-11). Time points depicted as 0, 14 and 21 days of aging. All AFM samples were deposited at a total peptide concentration of 10 µM.

The self-assembly of **ILVAGK** was altered by the presence and increasing concentration of DNA-peptide conjugates (Fig. 2b). With 0.1 equivalents of **A'-ILVAGK** the appearance of network-like structures was now not observed until 21 days of aging. The structures prior to that point also differ from those seen in the pure **ILVAGK** sample, they appeared to be less ordered and the network-like structure with a height between 1 and 2 nm, (21 days aging) in the 0.1 equiv sample was more densely interlinked in comparison to the pure **ILVAGK** sample (14 days). Self-assembly differed again with equimolar **A'-ILVAGK**. At 0 and 14 days of aging fibre-like structures were produced with heights between 0.5-3 nm (0 days) and 0.5-2 nm (14 days) respectively (Fig. 2c). These fibre-like structures lead to the formation of a very large structure at 21 days of aging which appeared to be built up of striated sheets. This may be due to crosslinking between structures similar to those observed in β-sheet forming peptides,[31] with a height ranging between 1 and 6 nm across the whole structure. It could be inferred that the addition of DNA-peptide conjugates into the peptide system slows the overall self-assembly of **ILVAGK**, possibly because the DNA partially inhibits the peptide monomers from coming together because of their size, preventing formation of kinetically trapped disordered structures and instead promote more ordered, equilibrium structures.

Study 1 therefore established that peptide driven self-assembly is altered with the addition of DNA-peptide conjugates, changing both the type of structures and the timescales on which they appear. To further explore the role of DNA within this system DNA hybridisation was introduced as another level of supramolecular chemistry which could indirectly affect the peptide-driven self-assembly.

Study 2 explored the effect of adding DNA hybridisation to the peptide-driven self-assembly. To achieve this, **A-ILVAGK** was mixed with DNA strands which were 1, 2, and 3 complements long (**A'**, **2A'** and **3A'** respectively, see ESI for sequences). With a single complement (i.e. using **A'**), it was anticipated that the self–assembly would differ from that observed in Study 1 due to the rigidity of dsDNA relative to ssDNA, as well as by the increased negative charge density. With multimeric-complement strands, it was expected that the DNA would either crosslink or deform the peptide assemblies, since we would have **2A'** and **3A'** each fully hybridised with 2 or 3 instances of **A-ILVAGK**, resulting in a DNA double helix decorated with 2 or 3 peptides, which would tend of their own arrangement. By interfacing the DNA and peptide assembly indirectly, we enabled hierarchical and emergent supramolecular behaviour. This is of interest as systems with hierarchy show unusual properties when compared with their component parts. For example, the Stupp lab have used DNA-peptide conjugates to produce structures similar to those expressed in the extracellular matrix of cells.[32]

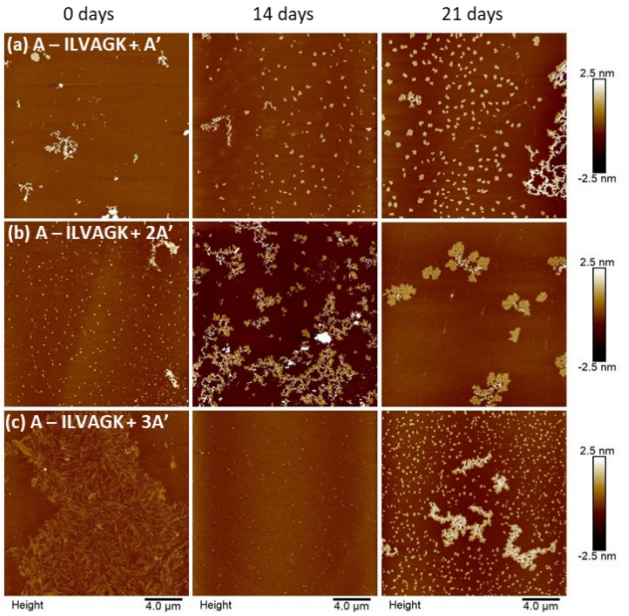

Figure 3. AFM images showing change in self-assembly of hybridised **A-ILVAGK** DNA-peptide conjugate and extended complements **A'** (a), **2A'** (b) and **3A'** (c), during 28 days of aging in TAMg buffer (see also Fig S.14-16). Time points depicted as 0, 14 and 21 days of aging. All AFM was carried out at a concentration of 10 µM.

A-ILVAGK + A' (1:1 equiv), **A–ILVAGK + 2A'** (2:1 equiv) and **A–ILVAGK + 3A'** (3:1 equiv) were heat-cooled from 55 °C for 10 mins, 35 °C for 20 mins, cooled to 4 °C in TAMg buffer to ensure correct hybridisation (melting temperature can be found in the ESI). Samples were aged and analysed as in Study 1. DLS measured a general increase in apparent diameter over the time period (Fig. S12) whereas CD spectroscopy showed both features for DNA and peptide, and remained stable over the period (Fig. S13). Again, AFM was more indicative of change. **A-ILVAGK + A'** 0 days of aging (Fig. 3a) produced a few fractal-like structure with a height of 2.5-5 nm; after 14 days of aging there were fewer of these fractal-like structures and more flakes, with a height and diameter of 2.9 ± 5.6 nm and 306 ± 75 nm respectively. At 21 days of aging, we observed a large fractal-like network (H: 1.5-3 nm) with more flakes (H: 1.9 ± 0.4 nm D: 379.3 ± 113.4 nm) visible on the surface. The appearance of flakes after 14 days of aging, may suggest the presence of a DNA double helix has improved the ability of the peptide to self-assembly, compared to the 1:1 doping of **ILVAGK** with **A'-ILVAGK** for the same time point (Fig. 2c), i.e. the double stranded DNA made self-assembly more closely resemble that of the pure peptide (Fig. 2a). This may be because DNA interference with **ILVAGK** self-assembly was reduced by making the DNA component rigid in its double helical form. However, by hybridising two conjugates to **2A'** we then increased the complexity and rigidity of the system. This was evidenced by the changes in self-assembly over the aging time frame for **A–ILVAGK + 2A'** and **3A'** respectively, in Fig. 3b/c. Doubling the length of the DNA helix (**2A'**), introduced a second instance of peptide from which crosslinking or assembly could occur. From Fig. 3b we can see that at 0 days of aging for **A-ILVAGK + 2A'** we observe a surface covered in small flakes (H: 4.3 ± 4.7 nm and D: 226.9 ± 4.8 nm). These structures grew into

network-like self-assemblies (H: 1.5-3 nm) at 14 days of aging (Fig. 3). At 21 days of aging these network-like structures appeared to break down into smaller fractal-like self-assemblies, with a height between 0.5-1.5 nm at the edges and 2.5-4 nm at the centre. In contrast, the self-assembly observed in Fig. 3c for **A-ILVAGK + 3A'** was very different to that observed as yet. At 0 days of aging, we observed a densely covered surface with fibre-like structures, with a height between 0.5 and 1 nm. This, in contrast to the previous two samples shows a breakdown into small dot-like structures at 14 days of aging, with a height between 3-4 nm (Fig. 3c), with growth into small flakes (H: 1.7 ± 0.4 nm and D: 284.5 ± 52.0 nm) and fractal-like self-assemblies with a height between 1 and 2.5 nm, at 21 days of aging. The reversal, over time in the standard growth from smaller to larger structures is particularly interesting for this sample set. It is possible that further extending the double helix to three lengths increased the dynamics within the system. We had expected that by rigidifying and extending the DNA component of the system there would be either crosslinking between self-assemblies or deformation of them. The reversal of the growth previously observed could be inferred as to support both outcomes: deformation, certainly, as the appearance of fibre-like structures was not previously observed. This may also suggest that there was a change in the crosslinking within this system.

Study 2 has shown that the addition of a rigid DNA double helix introduces a second level of self-assembly system which enhanced and changed the structures seen, previously driven only by peptidic self-association. The study highlights that seemingly well-defined structures as seen initially with **3A'** can be transient over longer timescales.

Study 3 was designed to clarify orthogonality present in our DNA–peptide conjugate system. Orthogonality of self-assembly within synthetic systems is currently of interest since it allows more sophisticated mimicry of natural systems.[33] If our system exhibits orthogonal behaviour this opens up opportunities for nanoscale controllability and complexity previously seen only in biological systems.[2] The difference in results between Study 1 and Study 2 show that we can control DNA-directed assembly by adding (or not adding) the appropriate complementary strands. By 'switching off' the peptide self-assembly pathway, while retaining the DNA hybridisation, we should be able to establish whether we have achieved orthogonality The sample set used for Study 3 was **A'–ILVAGK + A**. A buffer system which contained enough metal ions to support the formation of a DNA double helix but did not promote the self-assembly of **ILVAGK** was needed, and a 1 % sodium dodecyl sulphate (SDS) aqueous solution was identified as a medium which prevents self-assembly of peptides but does not denature the double helix.[34] Fig. 4a displays the CD spectra of the **A**/**A'** double helix in both TAMg and 1 % SDS buffer systems; it can be seen from the close similarity of these spectra that the double helix is intact in both buffer systems. In contrast, Fig. 4b has the CD spectra of **ILVAGK** in both buffer systems; it shows that **ILVAGK** adopts a β-turn formation in TAMg buffer, but is a random coil in 1 % SDS buffer. These CD spectra are stable over the full 28-day aging period and can be found in the ESI (Fig. S18), as was the apparent diameter measured by DLS for **A'-ILVAGK + A**, but not that for **ILVAGK** on its own (Fig. S17). Polyacrylamide gel electrophoresis (PAGE, Fig. 4c) in 1% SDS confirmed the presence of the DNA double helix in both the **A + A'** (lane 4) and **A'-ILVAGK + A** (lane 5) combinations. We can see from Figure 4c that both the samples, 4 and 5 ran at the same position on the gel when compared to the controls (single stranded DNA), **A** (lane 2) and **A'** (lane 3). The lack of higher molecular weight bands in Fig. 4c is also suggestive of the success in preventing the self-assembly of **ILVAGK**, this is further evidence to the integrity of the double helix in 1 % SDS buffer. AFM imaging showed that at 0 days of aging in 1% SDS, **ILVAGK** (Fig. 4d(i)) gave self-assembly similar to the network-like structures (H: 1-2 nm) seen in Study 1. This may be due to some self-assembly being established before treatment with SDS. The low percentage of SDS prevents further self-assembly of peptides but is less effective at breaking down already assembled structures. However, over the 28 days aging period we see the self-assembly change to small flake structures with an average height and diameter of 3.1 ± 7.2 nm and 296.9 ± 54.9 nm respectively at 7 days of aging, and further growth in diameter at 28 days of aging to an average height and diameter of 1.8 ± 0.6 nm and 363.9 ± 100.8 nm, respectively.

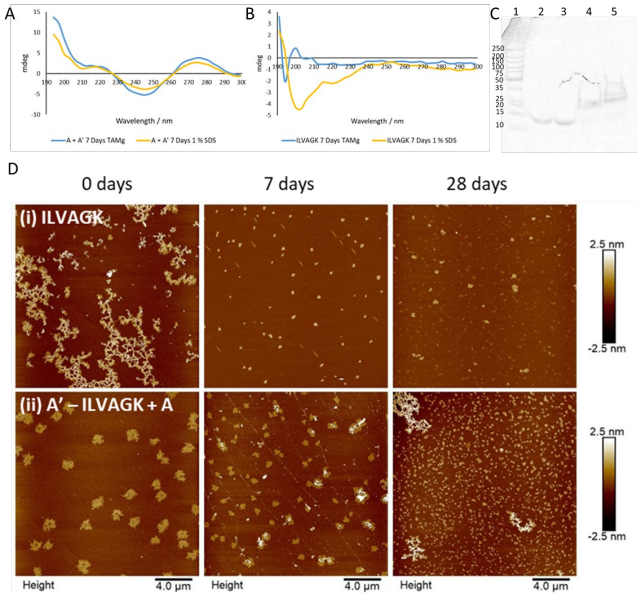

Figure 4. A: CD spectra showing DNA hybridisation of **A**, and **A'** is maintained in both TAMg and SDS buffer conditions. B: CD spectre showing **ILVAGK** self-assembly in TAMg and 1 % SDS conditions. In TAMg **ILVAGK** exhibits fibril formation, spectra are weak due to concentration of peptide. In 1 % SDS we observe random coil structure of **ILVAGK** due to denaturation by SDS. C: 12 % non-denaturing PAGE 1: Ladder, 2: Sequence **A (ss)**. 3: Sequence **A'(ss)**, 4: Sequence **A** + sequence **A'** hybridised in 1 % SDS (ds) and 5: Sequence **A** hybridised to **A'–ILVAGK** DNA–peptide conjugate in 1 % SDS (ds). Lack of larger bands indicate the successful prevention of ILVAGK DNA-peptide self-assembly. D: AFM images showing change in self-assembly of **ILVAGK** (i) and hybridised **A'-ILVAGK** DNA-peptide conjugate (ii) in 1 % sodium dodecyl sulphate, over 28 days of aging. Time points depicted as 0, 7 and 28 days of aging. All AFM, CD and PAGE were carried out at a concentration of 10 µM.

0 days of aging we observed large flakes (H: 1.5 ± 0.1 nm and D: 1.0 ± 0.1 μm), which at 7 days of aging shrank in height to an average of 1 nm for the flatter flakes with an average diameter of 505.2 ± 234.3 nm) and an average height of 18.1 ± 12.4 nm for the layered flakes although, maintained the same morphology. These structures further devolved to small flakes at 28 days of aging, with an average height and diameter of 1.8 ± 1.8 nm and 282.5 ± 120.6 nm, respectively (Fig. 4d(ii)). Although the size of these structures did change their morphology is alike. We believe that this lack of diverse self-assembly when compared to that observed in Study 2 (**A-ILVAGK + A'**, Fig. 3a), shows that we can switch each interaction on and off independently, giving orthogonality. Since the DNA- and peptide-driven associations do not directly interact, the new structures emerging from Study 2 are likely to arise from hierarchical or emergent assembly. Study 3 has shown that we are able to turn on and off peptide self-assembly using SDS, as well as turn on DNA self-assembly by adding and removing DNA complements. This control has also allowed us to confirm the presence of hierarchical self-assembly within our system.

Conclusion

By combining a self-assembling peptide with an oligonucleotide capable of hybridising with its complementary strand, we have created a doubly functional biomacromolecular hybrid. We have shown that the supramolecular chemistry of peptide and oligonucleotide segments can be operated independently, and thus the system displays orthogonality. This is not to say that the two regimes do not influence each other – presence of the oligonucleotide segment changes the rate of formation and eventual outcome of the resultant nanostructures. Moreover, when both peptide and oligonucleotide assembly 'are switched on,' the kinetics and thermodynamics of the system are again changed as these two systems interact indirectly (i.e., not through direct molecular contact of peptide and DNA fragments). Such indirect effects can be called 'emergent' in the sense that they operate only at the level of the conjugates, rather than at the level of the individual DNA and peptide components. Emergent assembly like this is widespread in nature, and this system provides an opportunity to further explore the possibilities of more nature-like self-assembly of functional nanostructures. The dynamic component of this work is also important: peptide and DNA nanostructures can be dynamic, even after annealing, and it is important that future development of these technologies take this aspect into account.

Acknowledgments

This work is supported by The Leverhulme Trust (grant No. RPG-2017-188). PGG thanks the European Commission for a Marie Skłodowska-Curie Individual Fellowship (842971 PepDNA-4D). MRR thanks the University of Vienna for financial support. All authors thank Kevin Howland for assistance with mass spectrometry and Wei-Feng Xue for assistance with atomic force microscopy.

Conflicts of interest

None to declare.

References

1. Buchberger, A., Simmons, C. R., Fahmi, N. E., Freeman, R. & Stephanopoulos, N. Hierarchical Assembly of Nucleic Acid/Coiled-Coil Peptide Nanostructures. *J. Am. Chem. Soc.* **142**, 1406–1416 (2020).

2. Higashi, S. L., Rozi, N., Hanifah, S. A. & Ikeda, M. Supramolecular architectures of nucleic acid/peptide hybrids. *International Journal of Molecular Sciences* vol. 21 1–25 (2020).

3. Lombardo, D., Calandra, P., Pasqua, L. & Magazù, S. Self-assembly of Organic Nanomaterials and Biomaterials: The Bottom-Up Approach for Functional Nanostructures Formation and Advanced Applications. *Mater. (Basel, Switzerland)* **13**, (2020).

4. Wang, L., Gong, C., Yuan, X. & Wei, G. Controlling the self-assembly of biomolecules into functional nanomaterials through internal interactions and external stimulations: A review. *Nanomaterials* **9**, (2019).

5. Macculloch, T., Buchberger, A. & Stephanopoulos, N. Emerging applications of peptide-oligonucleotide conjugates: Bioactive scaffolds, self-assembling systems, and hybrid nanomaterials. *Organic and Biomolecular Chemistry* vol. 17 1668–1682 (2019).

6. Cheng, Y. *et al.* A Multifunctional Peptide-Conjugated AIEgen for Efficient and Sequential Targeted Gene Delivery into the Nucleus. *Angew. Chemie* **131**, 5103–5107 (2019).

7. Basavalingappa, V. *et al.* Mechanically rigid supramolecular assemblies formed from an Fmoc-guanine conjugated peptide nucleic acid. *Nat. Commun.* **10**, (2019).

8. Kim, J., Narayana, A., Patel, S. & Sahay, G. Advances in intracellular delivery through supramolecular self-assembly of oligonucleotides and peptides. *Theranostics* vol. 9 3191–3212 (2019).

9. Jiang, T. *et al.* Structurally Ordered Nanowire Formation from Co-Assembly of DNA Origami and Collagen-Mimetic Peptides. *J. Am. Chem. Soc.* **139**, 14025–14028 (2017).

10. Datta, D., Tiwari, O. & Gupta, M. K. Self-Assembly of Diphenylalanine-Peptide Nucleic Acid Conjugates. *ACS Omega* **4**, 10715–10728 (2019).

11. Chen, L.-J. & Yang, H.-B. Construction of Stimuli-Responsive Functional Materials via Hierarchical Self-Assembly Involving Coordination Interactions. (2018) doi:10.1021/acs.accounts.8b00317.

12. Daly, M. L., Gao, Y. & Freeman, R. Encoding reversible hierarchical structures with supramolecular peptide-DNA materials. *Bioconjug. Chem.* **30**, 1864–1869 (2019).

13. Arrata, I. *et al.* Control of conformation in α-helix mimicking aromatic oligoamide foldamers through interactions between adjacent side-chains. *Org. Biomol. Chem.* **17**, 3861–3867 (2019).

14. Jin, J. *et al.* Peptide Assembly Directed and Quantified Using Megadalton DNA Nanostructures. *ACS Nano* **13**, 9927–9935 (2019).

15. Lou, C. *et al.* Peptide-oligonucleotide conjugates as nanoscale building blocks for assembly of an artificial three-helix protein mimic. *Nat. Commun.* **7**, (2016).

16. Stephanopoulos, N. Peptide-Oligonucleotide Hybrid Molecules for Bioactive Nanomaterials. *Bioconjug. Chem.* (2019) doi:10.1021/acs.bioconjchem.9b00259.

17. Stroo, E., Koopman, M., Nollen, E. A. A. & Mata-Cabana, A. Cellular regulation of amyloid formation in aging and disease. *Frontiers in Neuroscience* vol. 11 64 (2017).

18. Rodrigue, K. M., Kennedy, K. M. & Park, D. C. Beta-amyloid deposition and the aging brain. *Neuropsychology Review* vol. 19 436–450 (2009).

19. Hayden, E. Y. & Teplow, D. B. Amyloid β-protein oligomers and Alzheimer's disease. **5**, 1–11 (2013).

20. Morris, K. L. *et al.* Exploring the sequence–structure relationship for amyloid peptides. *Biochem. J.* **450**, 275–283 (2013).

21. Abraham, J. N., Gour, N., Bolisetty, S., Mezzenga, R. & Nardin, C. Controlled aggregation of peptide-DNA hybrids into amyloid-like fibrils. *Eur. Polym. J.* **65**, 268–275 (2015).

22. Rha, A. K. *et al.* Electrostatic Complementarity Drives Amyloid/Nucleic Acid Co-Assembly. *Angew. Chemie - Int. Ed.* **59**, 358–363 (2020).

23. Kedracki, D., Filippov, S. K., Gour, N., Schlaad, H. & Nardin, C. Formation of DNA-copolymer fibrils through an amyloid-like nucleation polymerization mechanism. *Macromol. Rapid Commun.* **36**, 768–773 (2015).

24. Loo, Y. *et al.* Peptide Bioink: Self-Assembling Nanofibrous Scaffolds for Three-Dimensional Organotypic Cultures. *Nano Lett.* **15**, 6919–6925 (2015).

25. Seow, W. Y. & Hauser, C. A. E. Short to ultrashort peptide hydrogels for biomedical uses. *Mater. Today* **17**, 381–388 (2014).

26. Seow, W. Y. & Hauser, C. A. E. Short to ultrashort peptide hydrogels for biomedical uses. *Materials Today* vol. 17 381–388 (2014).

27. Mishra, A. *et al.* Ultrasmall natural peptides self-assemble to strong temperature-resistant helical fibers in scaffolds suitable for tissue engineering. *Nano Today* **6**, 232–239 (2011).

28. Su, Y. C. *et al.* Azide-alkyne cycloaddition for universal post-synthetic modifications of nucleic acids and effective synthesis of bioactive nucleic acid conjugates. *Org. Biomol. Chem.* **12**, 6624–6633 (2014).

29. Fantoni, N. Z., El-Sagheer, A. H. & Brown, T. A Hitchhiker's Guide to Click-Chemistry with Nucleic Acids. *Chemical Reviews* (2021) doi:10.1021/acs.chemrev.0c00928.

30. Zhang, G. *et al.* Morphology Diagram of Single-Layer Crystal Patterns in Supercooled Poly(ethylene oxide) Ultrathin Films: Understanding Macromolecular Effect of Crystal Pattern Formation and Selection. **11**, 46 (2021).

31. Uchida, N. & Muraoka, T. Current Progress in Cross-Linked Peptide Self-Assemblies. *Mol. Sci.* (2020) doi:10.3390/ijms21207577.

32. Stephanopoulos, N. *et al.* Bioactive DNA-Peptide Nanotubes Enhance the Differentiation of Neural Stem Cells Into Neurons. (2014) doi:10.1021/nl504079q.

33. Ariga, K. *et al.* Nanoarchitectonics beyond Self-Assembly: Challenges to Create Bio-Like Hierarchic Organization. *Angewandte Chemie - International Edition* vol. 59 15424–15446 (2020).

34. Lipfert, J., Doniach, S., Das, R. & Herschlag, D. Understanding nucleic acid-ion interactions. *Annual Review of Biochemistry* vol. 83 813–841 (2014).